Journal of Cluster Science, Vol. 7, No. 1, 1996

Aurated Tungsten–Triosmium Cluster Compounds. Synthesis and Characterization of $LWOs_3(CO)_{12}(AuPPh_3)$ and Related Hydrogenation Products $LWOs_3(CO)_{11}(\mu\text{-}H)_2(AuPPh_3)$, $L = C_5H_5$ and C_5Me_5

Chi-Jung Su,[1] Yun Chi,[1,3] Shie-Ming Peng,[2] and Gene-Hsiang Lee[2]

Received August 17, 1995

Two heterometallic compounds $LWOs_3(CO)_{12}(AuPPh_3)$, $L = Cp$ (**6**); $L = Cp^*$ (**7**), were prepared by *in-situ* generation of clusters $[LWOs_3(CO)_{12}][PPh_4]$ from $Os_3(CO)_{10}(NCMe)_2$ and $[LW(CO)_3][PPh_4]$, followed by addition of Ph_3PAuCl. These derivatives possess a tetrahedral Os_3W core in which the $AuPPh_3$ unit bridges an Os–Os edge and the unique bridging CO ligand spans the opposite Os–W edge. Crystal data for **6**: space group $P\bar{1}$; $a = 9.328(3)$, $b = 13.745(3)$, $c = 16.231(3)$ Å, $\alpha = 115.00(2)$, $\beta = 97.27(2)$, $\gamma = 90.17(2)°$, $Z = 2$; final $R_F = 0.045$, $R_{wF} = 0.044$ for 4049 reflections with $I > 2\sigma(I)$. Crystal data for **7**: space group $P2_1/n$; $a = 9.775(2)$, $b = 17.106(4)$, $c = 25.074(3)$ Å, $\beta = 91.10(1)°$, $Z = 4$; final $R_F = 0.035$, $R_{wF} = 0.028$ for 4196 reflections with $I > 2\sigma(I)$. Hydrogenation of **6** and **7** afforded the respective dihydride complexes $LWOs_3(CO)_{11}(\mu\text{-}H)_2(AuPPh_3)$, (**8**) $L = Cp$; (**9**), $L = Cp^*$ in moderate yields. Their dynamic processes in solution were also established by ^1H, ^{13}C and, ^{31}P NMR spectroscopies.

KEY WORDS: Heterometallic cluster; osmium; tungsten; triphenylphosphine; gold; carbonyl; hydride.

INTRODUCTION

Skeletal rearrangement of cluster compounds constitutes an important research topic because it provides realistic models of the metal–metal and the ligand–metal interactions on catalytic metal surfaces [1]. Along this

[1] Department of Chemistry, National Tsing Hua University, Hsinchu 30043, Taiwan.
[2] Department of Chemistry, National Taiwan University, Taipei 10764, Taiwan.
[3] To whom all correspondence should be addressed.

1040-7278/96/0300-0085$09.50/0

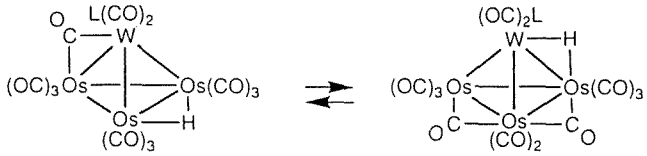

L = Cp, **1a** **1b**
L = Cp*, **2a** **2b**

Scheme 1

research direction, we placed our special emphasis on the studies of the crystal structures and solution dynamics of tetranuclear clusters with empirical formula $LWOs_3(CO)_{12}(\mu\text{-H})$, (**1**) $L = C_5H_5$; (**2**) $L = C_5Me_5$ [2], $LWRu_3(CO)_{12}(\mu\text{-H})$, (**3**) $L = C_5H_5$; (**4**) $L = C_5M_5$ [3], and $Cp^*MoRu_3(CO)_{12}(\mu\text{-H})$ (**5**) [4]. These complexes were chosen because they were expected to provide a robust metallic framework, and by varying the transition metal atoms and the ancillary ligands, we could obtain a series of cluster compounds with diverse electronic and steric properties, which allowed us to investigate the bonding of the carbonyl ligands in the multimetallic coordination sphere and the concurrent reorganization of the structure of the cluster.

Our continuous efforts in this area have provided substantial new evidence about the μ_4-η^2-bonding of the carbonyl ligand vs. cluster framework isomerization, which complement the framework isomerization and formation of μ_4-CO found in the $[HFe_4(CO)_{13}]^-$ system [5]. For example, we discovered that both WOs_3 clusters **1** and **2** adopt a tetrahedral metal framework in which the hydride ligand bridges different metal–metal

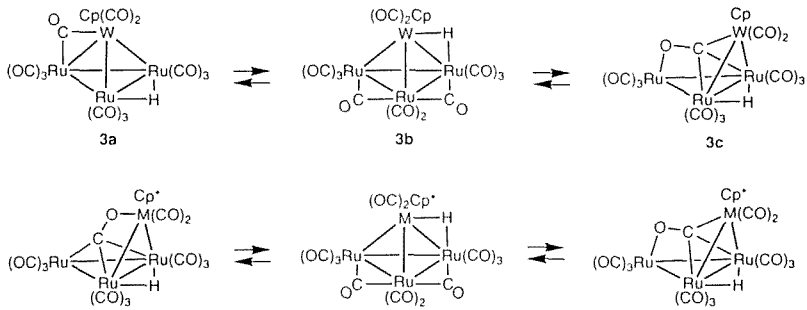

3a 3b 3c

M = W, **4a** **4b** **4c**
M = Mo, **5a** **5b** **5c**

Scheme 2

bonds: one bridges an Os–Os edge and the second occupies a W–Os edge, implying the existence of two interconvertible isomers (Scheme 1). However, for the analogous WRu_3 and $MoRu_3$ derivatives **3–5**, we observed the formation of butterfly derivatives generated via reversible cleavage of a W–Ru (or Mo–Ru) bond, and the conversion of one CO ligand into a novel μ_4-η^2-mode (Scheme 2). The butterfly isomers were unambiguously identified by structural analyses and the ^{13}C NMR spectroscopic data.

As part of our continuing investigation on this subject, we prepared two additional WOs_3 clusters $LWOs_3(CO)_{12}(AuPPh_3)$, (**6**) $L = Cp$; (**7**), $L = Cp^*$, with an isolobal $AuPPh_3$ fragment formally replacing the bridging hydride ligand. In order to strengthen our understanding on the predicted molecular geometries under the influence of isolobal $AuPPh_3$ fragment, we carried out the X-ray crystal structural determinations as well as the ^{13}C NMR studies on these two complexes. In this paper, we report these results, and present the data on variable temperature NMR studies of hydride migration and intramolecular tautomerization of related hydrogenation products $LWOs_3(CO)_{11}(\mu\text{-}H)_2(AuPPh_3)$ (**8**) $L = Cp$; (**9**), $L = Cp^*$.

EXPERIMENTAL PROCEDURE

General Information and Materials. Infrared spectra were recorded on a Bomem M-100 FT-IR spectrometer. ^1H, ^{13}C, and ^{31}P NMR spectra were recorded on a Bruker AM-400 (400.13 MHz) or a AMX-300 (300.6 MHz) instrument. Chemical shifts are quoted with respect to internal standard tetramethylsilane (^1H and ^{13}C NMR) and external standard 85% H_3PO_4 (^{31}P NMR). Mass spectra were obtained on a JEOL-HX110 spectrometer operating in fast atom bombardment (FAB) mode. All reactions were performed under a nitrogen atmosphere using deoxygenated solvents dried with an appropriate reagent. The progress of reactions was monitored by analytical thin-layer chromatography (5735 Kieselgel 60 F_{245}, E. Merck) and the products were separated on commercially available preparative thin-layer chromatographic plates (Kieselgel 60 F_{254}, E. Merck). The elemental analyses were performed at the NSC Regional Instrument Center at National Cheng Kung University, Tainan, Taiwan.

Preparation of $CpWOs_3(CO)_{12}(AuPPh_3)$. Toluene (40 ml), acetonitrile (5 ml), and $Os_3(CO)_{10}(NCMe)_2$, freshly prepared from $Os_3(CO)_{12}$ (500 mg, 0.55 mmol) and anhydrous Me_3NO (91 mg, 1.21 mmol), were placed in a 100-ml flask. After the flask was placed a preheated oil bath at 110°C, a toluene solution (15 ml) of $[CpW(CO)_3][PPh_4]$ (372 mg,

0.55 mmol) was added dropwise over 5 minutes. The mixture was then heated to reflux for 3 hours, during which the color changed to red–brown. Then the solution was cooled to room temperature and the solvent removed under vacuum. The oily residue was dissolved in 40 ml of THF, followed by addition of $TlPF_6$ (116 mg, 0.33 mmol) and $ClAu(PPh_3)$ (164 mg, 0.33 mol) with vigorous stirring. The mixture was continuously stirred for 1 hour at room temperature. Then the solvent was removed and the residue was separated by thin-layer chromatography. Development with a 2:3 mixture of dichloromethane and hexane produced one red–brown band, which was removed from silica gel plates to yield 227 mg of $CpWOs_3(CO)_{12}(AuPPh_3)$ (**6**, 0.14 mmol, 26%) after recrystallization.

Spectral data for **6**: MS spectrum (FAB, ^{184}W, ^{192}Os, ^{197}Au), *m/z* 1620(M^+). IR(CCl_4): ν(CO), 2065(m), 2023(vs), 2010(vw), 1979(br, m), 1964(br, m) cm^{-1}. ^1H NMR ($CDCl_3$, 294 K): δ 7.48 to 7.44 (m, 15H), 5.29 (s, 5H). ^{31}P NMR ($CDCl_3$, 294 K): δ 74.1 (s). ^{13}C NMR (CD_2Cl_2, 193 K): CO, δ 197.6 (br, 7 C), 186.6 (d, $J_{P-C}=2$ Hz), 177.5 (d, $J_{P-C}=8$ Hz), 177.2 (s), 174.4 (d, $J_{P-C}=8$ Hz), 171.4 (s). Elemental analysis for $C_{35}H_{20}O_{12}PAuWOs_3$: Calcd: C, 26.03; H, 1.25. Found: C, 25.87; H, 1.30.

Preparation of $Cp^*WOs_3(CO)_{12}(AuPPh_3)$. The respective Cp* derivative $Cp^*WOs_3(CO)_{12}(AuPPh_3)$ was obtained in 41% yield from combination of $Os_3(CO)_{10}(NCMe)_2$ and $[Cp^*W(CO)_3][PPh_4]$ under analogous conditions, followed by addition of $ClAu(PPh_3)$ in the presence of $TlPF_6$.

Spectral data for **7**: MS spectrum (FAB, ^{184}W, ^{192}Os, ^{197}Au), *m/z* 1690(M^+). IR(C_6H_{12}): ν(CO), 2063 (s), 2023(vs), 2009(sh, vw), 1988(br, w), 1973(m), 1963(w), 1955(w), 1943(vw) cm^{-1}. ^1H NMR ($CDCl_3$, 294 K): δ 7.52 to 7.41 (m, 15H), 1.96 (s, 15H). ^{31}P NMR ($CDCl_3$, 294 K): δ 70.5 (s). ^{13}C NMR (CD_2Cl_2, 210 K): CO, δ 200.0 (br, 7C), 186.9 (s), 178.3 (d, $J_{P-C}=7$ Hz), 176.4 (s), 175.8 (s), 175.0 (d, $J_{P-C}=7$ Hz). Elemental analysis for $C_{40}H_{30}O_{12}PAuWOs_3$: Calcd: C, 28.51; H, 1.79. Found: C, 28.54; H, 1.82.

Hydrogenation of $CpWOs_3(CO)_{12}(AuPPh_3)$. The toluene solution (30 ml) of $CpWRu_3(CO)_{12}(AuPPh_3)$ (47 mg, 0.029 mmol) was refluxed under 1 atm of hydrogen for 6 hours. After the solution was cooled to room temperature, the solvent was evaporated *in vacuo* and the residue was separated by thin layer chromatography (dichloromethane:hexane = 2:3), giving 23 mg of red–orange $CpWOs_3(CO)_{11}(\mu\text{-}H)_2(AuPPh_3)$ (**6**, 0.014 mmol, 49%).

Spectral data for **8**: MS spectrum (FAB, ^{184}W, ^{192}Os, ^{197}Au), m/z 1594(M^+). IR(C_6H_{12}): ν(CO), 2090(w), 2078(w), 2070(m), 2031(s),

2019(vs), 2006(m), 1992(m), 1987(m), 1968(w), 1944(br, vw) cm^{-1}. ^1H NMR($CDCl_3$, 210 K): δ 7.48 to 7.36 (m, 15H), 5.30 (s, 5H, **a**, 55%), 5.09 (s, 5H, **b**, 45%), −17.58 (s, $J_{W-H}=46$ Hz, 1H, **b**), −20.39 (s, 2H, **c**), −20.48 (s, 1H, **b**), −22.25 (s, 2H, $J_{W-H}=43$ Hz, **a**). ^{31}P NMR ($CDCl_3$, 210K): δ 88.7 (s, **a**, 49%, 82.9 (s, **c**, 6%), 76.4 (s, **b**, 45%). Elemental analysis for $C_{34}H_{22}O_{11}PAuWOs_3$: Calcd: C, 25.70; H, 1.40. Found: C, 25.17; H, 1.48.

Hydrogenation of $Cp^*WOs_3(CO)_{12}(AuPPh_3)$. The toluene solution (30 ml) of $CpW^*Ru_3(CO)_{12}(AuPPh_3)$ (54 mg, 0.032 mmol) was refluxed under 1 atm of hydrogen for 12 hours. After the solution was cooled to room temperature, the solvent was evaporated *in vacuo* and the residue was separated by thin layer chromatography (dichloromethane:hexane = 2:3), giving 43 mg of red–orange $Cp^*WOs_3(CO)_{11}(\mu\text{-}H)_2(AuPPh_3)$ (**9**, 0.025 mmol, 80

Spectral data for **9**: MS spectrum (FAB, ^{184}W, ^{192}Os, ^{197}Au), 1664 *m/z* (M^+). IR(C_6H_{12}): ν(CO), 2069(s), 2028(vs), 2023(vs), 1996(br, m), 1982(w), 1935(w), 1929(vw) cm^{-1}. ^1H NMR ($CDCl_3$, 294 K): δ 7.62 to 7.45 (m, 15H), 2.05 (s, 15H, **b**, 8%), 1.95 (s, 15H, **a**, 92%), −19.03 (br, 1H, **b**, −20.95 (s, $J_{W-H}=43$ Hz, 2H, **a**), −21.07 (br, 1H, **b**). ^{31}P NMR ($CDCl_3$, 210 K): δ 86.8 (s, **a**, 92%), 80.1 (s, **b**, 8%). ^{13}C NMR (CD_2Cl_2, 180 K): CO, δ 210.3 (2C, $J_{W-C}=153$ Hz), 197.7 (d, 2 C, $J_{P-C}=5$ Hz), 185.4 (2C), 183.6, 173.9 (d, 2C, $J_{P-C}=10$ Hz), 171.7 (2C). Elemental analysis for $C_{39}H_{32}O_{11}PAuWOs_3$: Calcd: C, 28.23; H, 1.94. Found: C, 28.12; H, 1.99.

X-Ray Crystallography. Diffraction measurements were carried out on a Nonius CAD-4 diffractometer. Lattice parameters of **6** were determined from 25 randomly selected high angle reflections with 2θ angles in the range 18.68–25.32, whereas the corresponding cell dimensions of complex **7** were determined from 25 reflections, with 2θ angle in the range of 21.48–24.64. All reflections were corrected for Lorentz, polarization, and absorption effects. All data reduction and refinement were performed using the NRCC-SDP-VAX packages [6]. The structures were refined by full-matrix least squares, all non-hydrogen atoms were refined with anisotropic thermal parameters and the hydrogen atoms on organic ligands were calculated in idealized positions and included in the structure factor calculation. The combined data collection and refinement parameters are given in Table I. Atomic positional parameters for complex **6** are found in Table II, whereas some selected bond angles and lengths are given in Table IV. The corresponding parameters of **7** appear in Tables III and V, respectively.

Table I. Experimental Data for the X-ray Diffraction Studies[a]

	6	7
Empirical formula	$C_{35}H_{20}O_{12}P_1Au_1Os_3W$	$C_{40}H_{30}O_{12}P_1Au_1Os_3W$
Crystal system	triclinic	monoclinic
Space group	$P\bar{1}$	$P2_1/n$
a (Å)	9.328(3)	9.775(2)
b (Å)	13.745(3)	17.106(4)
c (Å)	16.231(3)	25.074(3)
α (°)	115.00(2)	
β (°)	97.27(2)	91.10(1)
γ (°)	90.17(2)	
Volume (Å^3)	1867.3(8)	4192(1)
Mol. wt.	1614.91	1685.06
Crystal size, mm	$0.20 \times 0.20 \times 0.40$	$0.20 \times 0.45 \times 0.55$
Z	2	4
D_c (g/cm^3)	2.872	2.670
$F(000)$	1444	3048
h, k, l ranges	-10 10, 0 14, -17 15	-10 10, 0 18, 0 26
μ(Mo–K$_\alpha$) mm^{-1}	17.32	15.44
Transmission factors	1.00, 0.70	1.00, 0.36
No. of unique data	4845	5474
Data with $I > 2\sigma(I)$	4049	4196
No. of parameters	479	524
R_F; R_w; G.O.F.	0.045; 0.044; 4.03	0.035; 0.028; 2.06
Maximum Δ/σ ratio	0.040	0.038
Residual electron, eÅ^{-3}	2.03/$-$2.44	1.44/$-$1.29

[a] Features common to all determinations: λ(Mo–K$_\alpha$) = 0.70930 Å; Nonius CAD-4 diffractometer; temperature, 297 K; $R = \sum ||F_o| - |F_c|| / \sum |F_o|$, $R_w = [\sum w(F_o - F_c)^2 / \sum wF_o^2]^{1/2}$; G.O.F. $= [\sum w |F_o - F_c|^2 / (N_o - N_v)]]^{1/2}$, $w^{-1} = \sigma^2(F)$. (N_o = number of observations; N_v = number of variables).

Table II. Atomic Coordinates and Equivalent Isotopic Displacement Coefficients for **6**

	x	y	z	Biso
Au	0.17803(11)	0.44020(7)	0.19734(7)	3.17(5)
Os1	0.39348(10)	0.59591(7)	0.31006(6)	2.48(5)
Os2	0.08921(11)	0.64565(8)	0.29635(7)	2.85(5)
Os3	0.31464(11)	0.80672(7)	0.35919(7)	2.66(5)
W	0.25471(11)	0.70240(7)	0.47586(6)	2.54(5)
P	0.0994(7)	0.2650(5)	0.1081(4)	2.9(3)

Table II. Continued

	x	*y*	*z*	Biso
C1	0.430(6)	0.565(3)	0.189(3)	14.7(36)
C2	0.450(3)	0.4649(20)	0.2995(15)	4.2(15)
C3	0.573(3)	0.6551(20)	0.3588(18)	5.2(16)
C4	0.010(3)	0.6022(20)	0.1696(18)	5.1(16)
C5	−0.041(3)	0.5454(20)	0.3003(19)	5.2(16)
C6	−0.0240(24)	0.7573(18)	0.3400(16)	3.6(14)
C7	0.239(3)	0.772(3)	0.2317(22)	7.5(24)
C8	0.489(2)	0.8719(21)	0.3505(19)	4.7(17)
C9	0.216(3)	0.9271(18)	0.4024(16)	3.8(14)
C10	0.4258(23)	0.8302(22)	0.4840(17)	4.3(17)
C11	0.437(3)	0.6501(18)	0.5044(16)	3.6(14)
C12	0.2045(23)	0.5537(18)	0.4230(16)	3.5(13)
C13	−0.094(3)	0.2403(20)	0.1014(16)	4.3(16)
C14	−0.160(3)	0.1669(20)	0.1271(16)	4.6(16)
C15	−0.301(3)	0.157(3)	0.1233(21)	6.6(23)
C16	−0.390(3)	0.215(3)	0.0942(21)	7.3(24)
C17	−0.334(3)	0.293(3)	0.0667(23)	7.7(22)
C18	−0.188(3)	0.3036(23)	0.0707(19)	6.0(20)
C19	0.1319(24)	0.2093(18)	−0.0120(14)	3.2(13)
C20	0.051(3)	0.1258(19)	−0.0788(16)	4.0(14)
C21	0.084(3)	0.0788(23)	−0.1669(18)	6.6(19)
C22	0.200(3)	0.1192(22)	−0.1871(18)	5.6(19)
C23	0.284(3)	0.206(3)	−0.1227(20)	7.0(22)
C24	0.251(3)	0.2563(1)	−0.0316(18)	5.0(16)
C25	0.1832(24)	0.1731(16)	0.1540(15)	3.1(12)
C26	0.244(3)	0.0807(19)	0.1017(16)	3.9(14)
C27	0.315(3)	0.0197(20)	0.1405(19)	5.4(18)
C28	0.327(3)	0.0472(21)	0.2288(20)	5.9(19)
C29	0.262(3)	0.1372(22)	0.2838(18)	5.7(18)
C30	0.191(3)	0.2023(19)	0.2484(17)	4.6(16)
C31	0.088(3)	0.7009(22)	0.5687(18)	6.5(18)
C32	0.057(3)	0.7922(23)	0.5446(17)	5.6(18)
C33	0.146(3)	0.849(3)	0.5713(20)	6.6(21)
C34	0.262(3)	0.834(3)	0.6260(18)	9.4(22)
C35	0.217(6)	0.733(4)	0.624(3)	16.3(46)
O1	0.450(3)	0.5577(16)	0.1182(14)	10.7(19)
O2	0.4986(20)	0.3805(13)	0.2928(12)	5.3(11)
O3	0.6972(19)	0.6885(15)	0.3951(15)	7.0(14)
O4	−0.032(3)	0.5814(16)	0.0925(12)	8.6(16)
O5	−0.1293(22)	0.4924(16)	0.3130(17)	8.5(16)
O6	−0.1014(18)	0.8338(13)	0.3684(12)	4.8(11)
O7	0.2233(23)	0.7603(17)	0.1581(12)	7.9(14)
O8	0.5961(22)	0.9087(16)	0.3459(17)	8.7(17)
O9	0.1536(20)	1.0093(13)	0.4302(13)	5.7(12)
O10	0.5232(19)	0.8818(14)	0.5413(12)	5.6(12)
O11	0.5445(20)	0.6211(18)	0.5315(14)	7.5(16)
O12	0.1761(19)	0.4616(13)	0.4126(11)	5.3(11)

Table III. Atomic Coordinates and Equivalent Isotropic Displacement coefficients for **7**

	x	*y*	*z*	Biso
Au	0.87597(6)	0.22640(4)	0.01285(3)	2.95(3)
Os1	0.93790(6)	0.34914(4)	0.08210(3)	2.29(3)
Os2	0.75163(6)	0.22580(4)	0.11311(3)	2.33(3)
Os3	0.91116(6)	0.30167(4)	0.19054(3)	2.51(3)
W	0.69213(6)	0.39023(4)	0.13898(3)	2.31(3)
P	0.9046(4)	0.1727(3)	−0.06933(17)	2.77(22)
C1	1.0388(14)	0.4327(9)	0.1146(6)	3.0(8)
C2	0.9335(16)	0.3951(10)	0.0143(7)	4.3(10)
C3	1.1052(16)	0.2949(12)	0.0659(7)	5.0(11)
C4	0.6275(17)	0.2001(11)	0.0581(7)	4.8(10)
C5	0.8827(14)	0.1444(9)	0.1136(7)	3.2(8)
C6	0.6426(15)	0.1766(9)	0.1641(7)	3.5(9)
C7	1.0771(15)	0.2518(10)	0.1755(7)	4.2(9)
C8	0.8851(14)	0.2338(11)	0.2474(7)	4.2(9)
C9	1.0019(16)	0.3798(10)	0.2307(7)	4.2(9)
C10	0.6990(14)	0.3273(9)	0.2101(7)	3.3(8)
C11	0.5845(17)	0.3738(9)	0.0610(8)	4.6(10)
C12	0.5285(15)	0.3251(10)	0.1323(7)	3.6(8)
C13	0.8376(14)	0.2352(9)	−0.1222(6)	2.5(7)
C14	0.8978(15)	0.2411(10)	−0.1713(6)	3.8(9)
C15	0.8380(17)	0.2868(12)	−0.2114(7)	5.6(11)
C16	0.7234(18)	0.3281(13)	−0.2002(8)	6.4(12)
C17	0.6630(16)	0.3251(11)	−0.1519(8)	5.0(10)
C18	0.7206(16)	0.2783(11)	−0.1129(7)	4.8(10)
C19	0.8169(14)	0.0791(9)	−0.0814(6)	2.7(8)
C20	0.7657(16)	0.0580(9)	−0.1301(7)	3.8(9)
C21	0.7042(18)	−0.0137(10)	−0.1354(7)	4.9(10)
C22	0.6958(16)	−0.0633(10)	−0.0952(8)	4.7(10)
C23	0.7421(19)	−0.0439(11)	−0.0467(8)	6.0(12)
C24	0.8099(17)	0.0291(10)	−0.0384(7)	4.4(10)
C25	1.0874(14)	0.1582(9)	−0.0851(6)	3.0(8)
C26	1.1340(15)	0.0863(10)	−0.1013(7)	4.2(9)
C27	1.2728(18)	0.0759(12)	−0.1087(8)	5.8(11)
C28	1.3603(18)	0.1382(13)	−0.1040(8)	6.3(12)
C29	1.3123(16)	0.2070(12)	−0.0851(8)	6.2(12)
C30	1.1779(16)	0.2181(10)	−0.0773(8)	4.9(10)
C31	0.6678(16)	0.5219(9)	0.1117(6)	3.5(8)
C32	0.5359(15)	0.4895(10)	0.1229(6)	3.3(8)
C33	0.5303(16)	0.4726(10)	0.1784(7)	4.0(9)
C34	0.6578(16)	0.4921(10)	0.2029(7)	3.7(9)
C35	0.7398(16)	0.5245(9)	0.1616(7)	4.0(9)
C36	0.7134(17)	0.5573(10)	0.0610(7)	4.8(10)
C37	0.4211(17)	0.4862(12)	0.0820(8)	5.8(12)
C38	0.4062(16)	0.4460(12)	0.2099(7)	4.9(10)
C39	0.6934(18)	0.4921(11)	0.2607(7)	5.1(10)
C40	0.8738(17)	0.5691(11)	0.1739(8)	5.4(11)

Table III. Continued

	x	*y*	*z*	Biso
O1	1.1101(10)	0.4776(6)	0.1320(5)	4.5(6)
O2	0.9291(12)	0.4256(8)	−0.0275(5)	5.8(7)
O3	1.2037(10)	0.2679(8)	0.0529(6)	7.0(8)
O4	0.5457(12)	0.1792(8)	0.0240(5)	6.5(8)
O5	0.9618(12)	0.0938(7)	0.1169(5)	6.0(8)
O6	0.5780(11)	0.1407(7)	0.1934(5)	5.3(7)
O7	1.1782(11)	0.2168(8)	0.1688(5)	6.1(8)
O8	0.8714(11)	0.1904(8)	0.2823(5)	6.2(8)
O9	1.0546(12)	0.4276(7)	0.2558(6)	6.7(8)
O10	0.6322(10)	0.3100(7)	0.2495(4)	3.7(6)
O11	0.6392(10)	0.3741(7)	0.0157(4)	4.0(6)
O12	0.4231(11)	0.2950(8)	0.1297(6)	7.0(8)

Table IV. Selected Bond Distances (Å) and Bond Angles (°) of **6** (esd in Parentheses)

(A) metal–metal distances			
Os(1)–Os(2)	2.925(2)	Os(1)–Os(3)	2.790(2)
Os(2)–Os(3)	2.808(2)	Os(1)–W	2.937(2)
Os(2)–W	2.901(2)	Os(3)–W	2.918(1)
Au–Os(1)	2.775(2)	Au–Os(2)	2.786(1)
(B) metal–ligand distances			
Au–P	2.282(6)	Os(1)–C(1)	1.91(4)
Os(1)–C(2)	1.82(3)	Os(1)–C(3)	1.79(2)
Os(2)–C(4)	1.93(3)	Os(2)–C(5)	1.86(3)
Os(2)–C(6)	1.80(3)	Os(3)–C(7)	1.95(3)
Os(3)–C(8)	1.90(2)	Os(3)–C(9)	1.81(2)
Os(3)–C(10)	2.05(3)	W–C(10)	2.32(2)
W–C(11)	1.93(2)	W–C(12)	1.88(2)
W–C(31)	2.31(2)	W–C(2)	2.35(2)
W–C(33)	2.29(3)	W–C(34)	2.32(2)
W–C(35)	2.33(4)		
(C) metal–carbonyl ligand angles			
∠ Os(1)–C(1)–O(1)	173(3)	∠ Os(1)–C(2)–O(2)	174(2)
∠ Os(1)–C(3)–O(3)	174(2)	∠ Os(2)–C(4)–O(4)	175(2)
∠ Os(2)–C(5)–O(5)	171(2)	∠ Os(2)–C(6)–O(6)	179(2)
∠ Os(3)–C(7)–O(7)	166(2)	∠ Os(3)–C(8)–O(8)	178(2)
∠ Os(3)–C(9)–O(9)	178(2)	∠ Os(3)–C(10)–O(10)	143(2)
∠ W–C(10)–O(10)	133(2)	∠ W–C(11)–O(11)	172(2)
∠ W–C(12)–O(12)	163(2)		

RESULTS AND DISCUSSION

Synthesis of **6** *and* **7**. Complexes $LWOs_3(CO)_{12}(AuPPh_3)$, $L = C_5H_5$ (**6**) and C_5Me_5 (**7**), were prepared in moderate yields from condensation of $Os_3(CO)_{10}(NCMe)_2$ and salts $[LW(CO)_3][PPN]$ to generate the ionic tetrametallic clusters $[LWOs_3(CO)_{12}][PPN]$ [7] followed by addition of $ClAuPPh_3$ and chloride scavenger $TlPF_6$ [8]. Attempts to prepare cluster compounds **6** and **7** via addition of NaH to the respective hydride clusters $LWOs_3(CO)_{12}(\mu\text{-H})$ in THF, followed by addition of $ClAuPPh_3$ and $TlPF_6$, failed to afford the expected products.

These aurated cluster products were purified by thin-layer chromatography followed by recrystallization. They are all fairly soluble in common chlorinated solvents and the solutions are stable in air. The ^1H NMR spectra exhibit three phenyl resonances and the corresponding Cp and Cp* signals. The ^{31}P NMR spectroscopy is more informative and show the occurrence of only one singlet at δ 74.1 and 70.5 for complexes **6** and **7**, respectively. This result is in sharp contrast to that of hydride derivatives **1** and **2**; the latter exists in solution as two interconvertible isomers produced via hydride migration between Os–Os edge and W–Os edge (Scheme 1).

Crystal Structures of **6** *and* **7**. The molecular structure of **6** was determined from a single crystal X-ray diffraction study. An ORTEP diagram of **6** is shown in Fig. 1, and selected bond parameters are presented in Table IV. The metal core consists of a tetrahedral Os_3W arrangement. In this molecule, all metal–metal edges adopt variable bond lengths, in which the W–Os distances (2.937(2)–2.901(2) Å) are, on the average slightly longer than other Os–Os edges (2.925(2)–2.790(2) Å). The longest W–Os edge is the one that supports a slightly asymmetric bridging CO ligand (Os(3)–C(10) = 2.05(3) Å and W–C(10) = 2.32(2) Å), while the longest Os–Os edge, opposite to the W–Os(3) edge, is bridged by a $AuPPh_3$ fragment. The $AuPPh_3$ fragment is in the same plane as Os_3 triangle with dihedral angles 159.16(4)° (between the Os(1), Os(2), Os(3), and the Au, Os(1), Os(2) triangles) and 128.04(4)° (between the W, Os(1), Os(2), and the Au, Os(1), Os(2) triangles), respectively. In addition to the bridging carbonyl ligand CO(10), this molecule contains 11 terminal CO ligands, two CO ligands on the W atom and three CO ligands on each Os atom. Among 11 terminal CO ligands, two CO ligands adopt the semi-bridging mode; these semi-bridging CO ligands include the CO(7) ligand on Os(3) atom and the CO(12) ligand on W atom, these have nonlinear M–C–O angles in the range 166–163°. The observed WOs_3 core geometry is analogous to the previously determined crystal structure of **1** [2], in which the bridging hydride is located at the same position of the isolobal $AuPPh_3$ fragment.

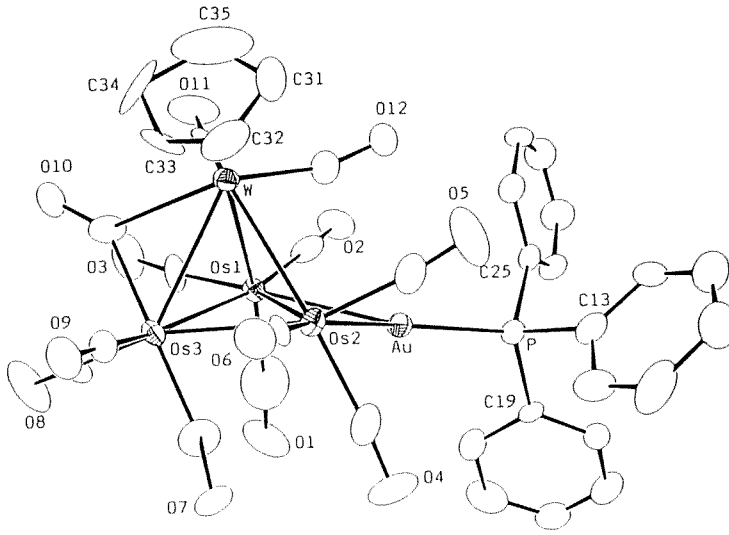

Fig. 1. Molecular structure of $CpWOs_3(CO)_{12}(AuPPh_3)$ (**6**), with numbering of atoms.

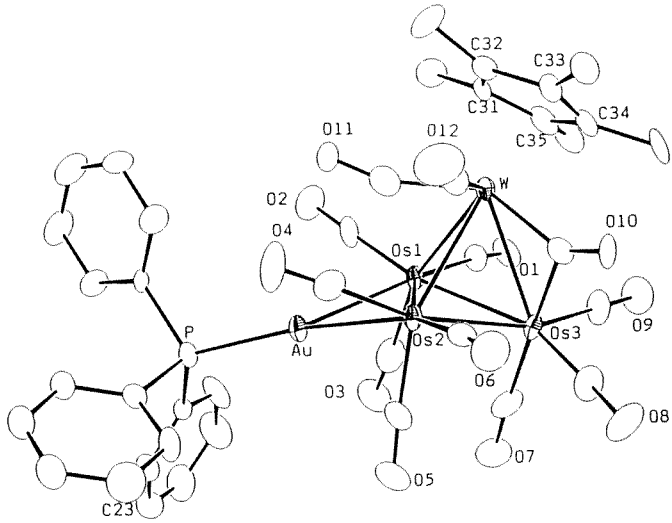

Fig. 2. Perspective drawing of $Cp^*WOs_3(CO)_{12}(AuPPh_3)$ (**7**) with numbering of atoms.

The Cp* derivative **7** was next examined by single-crystal X-ray analysis to illustrate the possible effect of the ancillary ligand on the solid structure. As indicated by the distances and angles given in Table V and the ORTEP diagram in Fig. 2, complex **7** is isostructural to that of the previously discussed Cp derivative **6**, exhibiting one bridging CO ligand on a W–Os edge and with the $AuPPh_3$ fragment attached to the opposite Os–Os edge. The variation of metal–metal distances is somewhat irregular but deviations between corresponding lengths are minimal ($\geq$0.05 Å). Comparison of the M–C–O angles in **7** with the respective angles in **6** shows the occurrence of semi-bridging interaction for CO(11) ligand on the tungsten atom and the removal of semi-bridging interaction for the axial CO(7) ligand on Os(3) atom.

The methyl groups of the Cp* ring are found to be pushed away from the WOs_3 core. The average displacement of the methyl groups from the ring plane defined by the inner carbon atoms is near 0.22 Å. This observed out-of-plane displacement of the methyl groups indicates steric repulsion

Table V. Selected Bond Distances (Å) and Bond Angles (deg) of **7** (esd in Parentheses)

(A) metal–metal distances			
Os(1)–Os(2)	2.902(1)	Os(1)–Os(3)	2.854(1)
Os(2)–Os(3)	2.790(1)	Os(1)–W	2.902(1)
Os(2)–W	2.947(1)	Os(3)–W	2.907(1)
Au–Os(1)	2.785(1)	Au–Os(2)	2.812(1)
(B) metal–ligand distances			
Au–P	2.278(4)	Os(1)–C(1)	1.91(1)
Os(1)–C(2)	1.87(2)	Os(1)–C(3)	1.93(2)
Os(2)–C(4)	1.87(2)	Os(2)–C(5)	1.89(2)
Os(2)–C(6)	1.88(2)	Os(3)–C(7)	1.88(2)
Os(8)–C(8)	1.86(2)	Os(3)–C(9)	1.89(2)
Os(3)–C(10)	2.18(1)	W–C(10)	2.08(2)
W–C(11)	1.98(2)	W–C(12)	1.95(2)
W–C(31)	2.36(2)	W–C(32)	2.32(2)
W–C(33)	2.35(2)	W–C(34)	2.40(2)
W–C(35)	2.41(2)		
(C) metal–carbonyl angles			
∠Os(1)–C(1)–O(1)	173(1)	∠Os(1)–C(2)–O(2)	178(2)
∠Os(1)–C(3)–O(3)	174(2)	∠Os(2)–C(4)–O(4)	176(2)
∠Os(2)–C(5)–O(5)	176(2)	∠Os(2)–C(6)–O(6)	174(2)
∠Os(3)–C(7)–O(7)	175(2)	∠Os(3)–C(8)–O(8)	178(2)
∠Os(3)–C(9)–O(9)	179(2)	∠Os(3)–C(10)–O(10)	131(1)
∠W–C(10)–O(10)	143(1)	∠W–C(11)–O(11)	159(1)
∠W–C(2)–O(12)	172(2)		

between the Cp* ring and nearby CO ligands. This enhanced steric interaction in **7** is further confirmed by the observation that (i) the C–W distances of the Cp* ligand (av. 2.37 Å) are much longer that those of the Cp ligand in 6 (av. 2.32 Å), and that (ii) the dihedral angle between the Os(1), Os(2), Os(3), and the Au, Os(1), Os(2) plane is reduced to 149.65(3)°, while the respective angle between the W, Os(1), Os(2), and the Au, Os(1), Os(2) plane expanded to 138.65(3)°.

^{13}C NMR Characterization. The variable temperature ^{13}C NMR spectra of **6** was recorded to show the dynamic motion of CO ligands in solution. At 193 K, the spectrum exhibits six intense signals at δ 197.6 (br), 186.6 (d, $J_{P-C} = 2$ Hz), 177.5 (d, $J_{P-C} = 8$ Hz), 177.2, 174.4 (d, $J_{P-C} = 8$ Hz) and 171.4, with ratio 7:1:1:1:1:1 (Fig. 3). The doublets at δ 177.5 and 174.4 are clearly caused by a three-bond J_{P-C} coupling to phosphorus atom in the PPh_3 ligand. Thus, they are assigned to the CO ligands (CO(3) and CO(6)) *trans* to the bridging $AuPPh_3$ fragment. For broad signal at δ 197.6, both the downfield chemical shift and the intensity ratio corresponding to seven CO ligands indicates that it comprises the bridging CO ligand CO(10), two W–CO ligands (CO(11) and CO(12)), and four terminal Os–CO ligands. We believe that the four Os–CO ligands are due to the CO(4), CO(5), CO(7), and CO(8) ligands (see Fig. 1), as all of them lie on the extension of the W–Os(2)–Os(3) triangular plane, and CO ligands with such coplanar arrangement tend to possess very low barriers for intermetallic CO migration [9]. In addition, all CO signals began to broaden and to collapse into the baseline at 240 K, then upon raising to 297 K, they turned into a broad signal at δ 189.5. This behavior is compatible to the existence of the rapid CO scrambling between all CO ligands on the coordination sphere.

Moreover, the ^{13}C NMR spectrum of **7** at 210 K shows a similar pattern of six peaks at δ 200.0 (broad, $7 \times CO$), 186.9, 178.3 ($J_{P-C} = 7$ Hz), 176.4, 175.8, 175.0 ($J_{P-C} = 7$ Hz). Upon raising to 294 K, the broad peak turns much sharper and moves to highfield region at δ 195.5, the second CO signal at δ 186.9 coalesces into the baseline, while the last four Os–CO ligands merge to form a broad lump at δ 173.2. This pattern of CO exchange indicates that complete scrambling among all 12 CO ligands in **7** is about to begin, which is in contrast to the previous observation on the Cp derivative **6**, where the rapid CO exchanges between all sites was clearly observable at room temperature.

Synthesis and Characterization of **8** *and* **9**. Hydrogenation of complexes **6** and **7** in refluxing toluene led to the formation of dihydride complexes $LWOs_3(CO)_{11}(\mu\text{-}H)_2(AuPPh_3)$ (**8**) $L = Cp$; (**9**) $L = Cp^*$, in moderate yields via elimination of one CO and addition of dihydrogen. Basically, these two

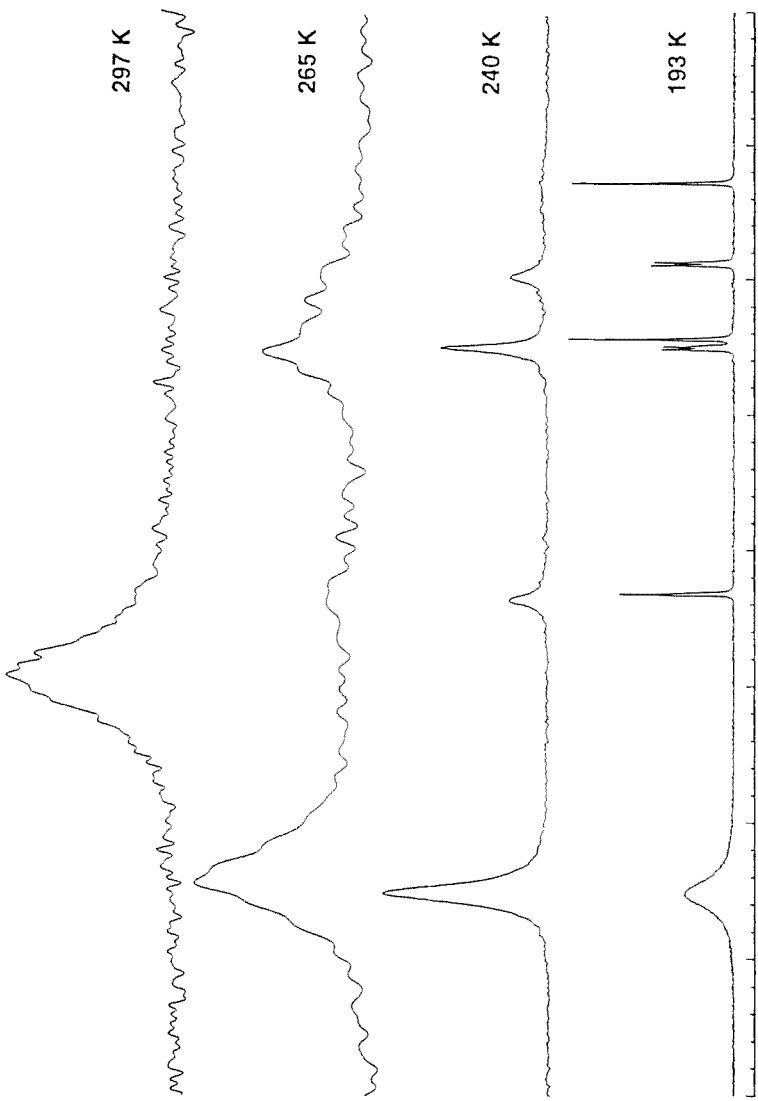

Fig. 3. Variable temperature ^{13}C NMR spectra of ^{13}CO-enriched (6) in CD_2Cl_2 solution, showing the region of CO resonances.

compounds show an essentially identical formulation with respect to corresponding WRu_3 derivatives $LWRu_3(CO)_{11}(\mu\text{-}H)_2(AuPPh_3)$ [10], but the location of hydrides and the solution fluxionality are somewhat different.

The key structural evidences of complex **8** were provided by NMR spectroscopies. The Cp derivative shows a broad signal at δ 79.0 in the ^{31}P NMR spectrum at room temperature. Upon lowering the temperature to 210 K, this broad signal became three signals at δ 88.7, 82.9, and 76.4 in an approximately 8.2:1:7.5 ratio, suggesting the presence of three isomers in solution. Consistent with the deduction of three interconvertible isomers, the ^1H NMR spectrum at 210 K shows four hydride signals at δ −17.58 ($J_{W-H}=46$ Hz), −20.39, −20.48, and −22.25 ($J_{W-H}=43$ Hz) in the ratio 4:1:4:8. The signals at δ −17.58 and −20.48 are immediately assigned to the hydrides of isomer **8b** (Scheme 3), which is analogous to that of derivatives $CpMoM_3(CO)_{11}(\mu\text{-}H)_3$, $M=$ Os and Ru [11], and is assigned according to their integration ratio and the observed J_{W-H} coupling of the first hydride signal. Furthermore, the second isomer is assigned to adopt the symmetrical structure **8a**, as it possesses only one hydride signal at δ −22.25 with coupling $J_{W-H}=43$ Hz. The least intense hydride signal at δ −20.39 is assigned to have another symmetric structure **8c** with both hydrides lying on the adjacent Os–Os edge. Similarly, the ^{31}P NMR signal at δ 82.9 is also assigned to this isomer due to its lowest relative intensity.

In contrast to the Cp derivative **8**, the Cp* derivative **9** at 210 K showed only two ^{31}P NMR signals at 86.8 and 80.1 in a ratio 9:1, indicating that the fluxional behavior in solution involves only two isomers and

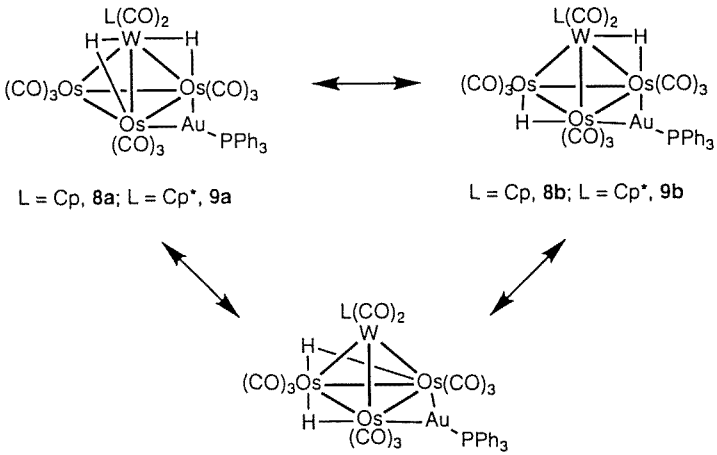

Scheme 3

is less complicated. The most abundant isomer appears to be symmetric derivative **9a**, as there is only one distinct hydride signal at δ −20.95 with coupling constant $J_{W-H} = 43$ Hz at 294 K, identical to that of the related trihydride derivative $Cp^*WM_3(CO)_{11}(\mu\text{-}H)_3$, M = Os or Ru [12]. On the other hand, the second, minor component **9b** showed two broad hydride signals at δ −19.03 and −21.07 at room temperature. Upon further lowering the temperature to 210 K, the hydride signal at δ −19.03 turned to much sharper and allowed us to observe the expected satellite peaks ($J_{W-H} = 48$ Hz). This feature agrees with the ^1H NMR pattern of the previously determined Cp derivative **8b**.

Furthermore, the ^{13}C NMR spectrum of **9** exhibits one W–CO signal at δ 210.3 ($J_{W-C} = 153$ Hz) and five Os–CO signals at δ 197.7 (d, $J_{P-C} = 5$ Hz), 185.4, 183.6, 173.9(d, $J_{P-C} = 10$Hz) and 171.7 in the ratio 2:2:1:2:2 at 210 K, revealing the presence of a plane of symmetry in isomer **9a**. Upon warming to 294 K, the CO signals at δ 185.4 and 183.6 with 2:1 ratio merge and coalesce into one sharp signal at δ 184.5, indicating that they are derived from the CO ligands on the unique $Os(CO)_3$ vertex, opposite the WOs_2 triangle that supports the hydrides and the $AuPPh_3$ fragment. The CO signals of minor isomer **9b** were not observed under this condition, apparently because of more rapid CO scrambling in **9b**.

Summary. The WOs_3 derivatives **6** and **7** exhibit a tetrahedral metal core in which the bridging CO ligand is associated with a W–Os edge and the $AuPPh_3$ fragment is linked to the opposite Os–Os edge. Their structures are identical to that of **1** with the $AuPPh_3$ fragment formally replacing the isolobal Os–H–Os hydride ligand. The isomer with $AuPPh_3$ fragment coordinated to the W–Os edge was not observed upon switching the ancillary ligand from Cp to Cp* (Scheme 4). We attribute that a sterically demanding nonbonding interaction between the phosphine on Au atom and the Cp* ligand on the W atom is the major factor that inhibits formation of this particular isomer. This speculation is akin to the conclusion of Salter and co-workers that steric interaction between the phosphine ligands

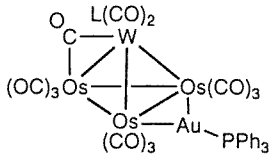

L = Cp, **6**
L = Cp*, **7**

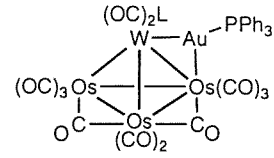

nonexistence

Scheme 4

attached to coinage metals in the clusters $[M_2Ru_4H_2(CO)_{12}(PR_3)_2]$, M = Cu, Ag, or Au; R = alkyl or aryl groups, can alter the cluster core geometries [13].

Furthermore, hydrogenation of **6** and **7** afforded the dihydride clusters **8** and **9** in moderate yields. Three isomers are detected for derivative **8**, which are produced by relocating the hydride ligands among the Os–Os and W–Os edges. The predominant symmetric isomer **a** possesses two equivalent W–H–Os hydride ligands, while the least abundant isomer **c** shows the existence of two Os–H–Os hydride ligands. When the Cp ligand in **8** is altered to the Cp* ligand in **9** the proportion of **a** increases and the proportions of both **b** and **c** decrease. This intramolecular hydride migration is well documented for trinuclear metal cluster compounds [14] and is also related to what has been reported for the anionic cluster complex $[Ru_4(CO)_{12}(\mu\text{-}H)_3]^-$ [15]. Moreover, the electron-donating ability of the Cp* ligand [16] may cause negative charge to accumulate on the W atom, which tends to attract the bridging hydride ligands to the W–Os edges and to increase the proportion of **a**, i.e., making the W–H–Os bond slightly more favorable than the Os–H–Os bond in terms of their small difference in bond energies. However, the contribution from the enhanced steric effect of the Cp* ligand cannot be completely ignored because there is no semi-bridging CO interaction in $Cp^*WRu_3(CO)_{11}(\mu\text{-}H)_3$ with respect to $CpWOs_3(CO)_{11}(\mu\text{-}H)_3$ and $CpMoRu_3(CO)_{11}(\mu\text{-}H)_3$ [11, 17], because of the unfavorable repulsion between W-bound CO ligands and Cp* fragment [12].

SUPPLEMENTARY MATERIAL AVAILABLE

A complete listing of thermal parameters, tables of nonessential bond distances and hydrogen atom coordinates for complexes **6** and **7** are available from one of the authors (Y.C.).

ACKNOWLEDGMENTS

We thank the National Science Council of the Republic of China (Grant No. NSC 85-2113-M007-008) for financial support and Mr. C. C. Chen for the experimental assistance.

REFERENCES

1. (a) R. D. Adams, T. S. Barnard, Z. Li, W. Wu, and J. Yamamoto (1994), *Organometallics* **13**, 2357; (b) R. D. Adams, T. S. Barnard, Z. Li, W. Wu, and J. Yamamoto (1994), *J. Am. Chem. Soc.* **116**, 9103; (c) J.-C. Wang, R.-C. Lin, Y. Chi, S.-M. Peng, and G.-H. Lee (1993), *Organometallics* **12**, 4061.

2. (a) M. R. Churchill, F. J. Hollander, J. R. Shapley, and D. S. Foose (1978), *J. Chem. Soc. Chem. Commun.* 534. (b) S.-M. Peng, G.-H. Lee, Y. Chi, C.-L. Peng, and L.-S. Hwang (1989), *J. Organomet. Chem.* **371**, 197.
3. Chi, F.-J. Wu, B.-J. Liu, C.-C. Wang, and S.-L. Wang (1989), *J. Chem. Soc. Chem. Commun.* 873.
4. Chi, C.-J. Su, L. J. Farrugia, S.-M. Peng, and G.-H. Lee (1994), *Organometallics* **13**, 4167.
5. (a) M. Manassero, M. Sansoni, and G. Longoni (1976), *J. Chem. Soc. Chem Commun.* 919; (b) C. P. Horwitz and D. F. Shriver (1984), *Adv. Organomet. Chem.* **23**, 219; (c) C. P. Horwitz and D. F. Shriver (1984), *Organometallics* **3**, 756; (d) C. P. Horwitz, E. M. Holt, C. P. Brock, and D. F. Shriver (1985), *J. Am. Chem. Soc.* **107**, 8136; (e) J. Wang, M. Sabat, C. P. Horwitz, and D. F. Shriver (1988), *Inorg. Chem.* **27**, 552.
6. E. J. Gabe, Y. LePage, J. P. Charland, F. L. Lee, and P. S. White (1989), *J. Appl. Crystallog.* **22**, 384.
7. M. Cazanoue, N. Lugan, J.-J. Bonnet, and R. Mathieu (1988), *Organometallics* **7**, 2480.
8. B. F. G Johnson, R. Khattar, J. Lewis, and P. R. Raithby (1989), *J. Chem. Soc. Dalton Trans.* 1421.
9. (a) A. Riesen, F. W. B. Einstein, A. K. Ma, R. K. Pomeroy, and J. A. Shipley (1991), *Organometallics* **10**, 3629; (b) J. Washington and J. Takats (1990), *Organometallics* **9**, 928.
10. C.-C. Chen, Y. Chi, S.-M. Peng, and G.-H. Lee (1993), *J. Chem. Soc. Dalton Trans.* 1823.
11. C. E. Housecroft, D. M. Matthews, A. L. Rheingold, and X. Song (1992), *J. Chem. Soc. Dalton Trans.* 2855; (b) L.-H. Hsu, W.-L. Hsu, D.-Y. Jan, and S. G. Shore (1986), *Organometallics* **5**, 1041.
12. Y. Chi, C.-Y. Cheng, and S.-L. Wang (1989), *J. Organomet. Chem.* **378**, 45.
13. (a) C. J. Brown, P. J. McCarthy, I. D. Salter, K. P. Armstrong, M. McPartlin, and H. D. Powell (1990), *J. Organomet. Chem.* **394**, 711; (b) C. J. Brown, P. J. McCarthy, and I. D. Salter (1990), *J. Chem. Soc. Dalton Trans.* 3583; (c) M. J. Freeman, A. G. Orpen, and I. D. Salter (1987), *J. Chem. Soc. Dalton Trans.* 379; (d) P. J. McCarthy, I. D. Salter, and V. Sik (1988), *J. Organomet. Chem.* **344**, 411; (e) P. J. McCarthy, I. D. Salter, and T. Adatia (1995), *J. Organomet. Chem.* **485**, 191.
14. (a) R.-C. Lin, Y. Chi, S.-M. Peng, and G.-H. Lee (1992), *Inorg. Chem.* **31**, 3818. (b) Y. Chi, B.-F. Chen, S.-L. Wang, R.-K. Chiang, and L.-S. Hwang (1989), *J. Organomet. Chem.* **377**, C59; (c) J. T. Park, Y. Chi, J. R. Shapley, M. R. Churchill, and J. W. Ziller (1994), *Organometallics* **13**, 813.
15. J. W. Koepke, J. R. Johnson, S. A. R. Knox, and H. D. Kaesz (1975), *J. Am. Chem. Soc.* **97**, 3947.
16. (a) F. P. Bordwell and M. P. Bausch (1983), *J. Am. Chem. Soc.* **105**, 6188. (b) E. J. Miller, S. J. Landon, and T. B. Brill (1985), *Organometallics*, **4**, 533.
17. M. R. Churchili and F. J. Hollander (1979), *Inorg. Chem.* **18**, 161.